2013 European Control Conference (ECC)
July 17-19, 2013, Zürich, Switzerland.

Stability Analysis of Droop Controlled Inverters via Dynamic Phasors and Contraction Theory

Valerio Mariani and Francesco Vasca

Abstract— **Droop techniques are widely used in distributed generation systems for the control of parallel inverters operating in grid-connected and islanded modes. Droop controllers without communication among the units are based on local measurements of active and reactive powers and usually allow the synchronization of the inverters to the common bus. On the other hand, instabilities can also occur. This paper investigates the stability of grid-connected droop controlled inverters by tackling the problem with a large signal perspective. A dynamic phasor model represented in a reference frame synchronous with the inverter voltage is proposed. The contraction theory applied to the model allows to determine an estimate of the domain of attraction of the stable equilibrium point. Simulation results demonstrate the effectiveness of the proposed analysis.**

I. Introduction

Modularity and flexibility are fundamental features for modern power (micro)grids which consist of a continuously increasing number and variety of different and distributed power sources and loads. In order to satisfy these properties the droop technique is a widely used control strategy for parallel inverters which connect the distributed generation units to the common bus.

The droop control technique has been proposed more than twenty years ago [1], and due to the recent growing interest on distributed generation systems it has received a renewed attention from the power systems and electronics engineering researchers. By restricting the state of the art to grid-connected topologies, good overviews on the topic can be found in [2], [3], [4], [5] and by consulting the references therein. On the other hand the control systems community has dedicated little efforts for a more theoretically rigorous analysis of the interesting issues related to the control and stability of distributed generation systems with droop control. At the best of our knowledge, within the major control journals and conferences, the only paper specifically dedicated to the topic is [6]. The major difficulty for the analysis of droop controlled inverters without communication among the different units, is due to the typical constraint that only "local" measurements are available. In that scenario it is fundamental to design a controller which allows the inverter synchronization with the grid. Indeed the synchronization underlies the proper power/load–sharing capabilities of droop controlled inverters [7]. The synchronization of grid-connected inverters is strictly related to the equilibrium point(s) stability of the dynamic system under droop control. The stability, so as the dynamic and steady state performance, of droop controlled inverters is significantly influenced by the line impedance and by the controller parameters [8], [9], [10]. The stability under droop control is typically analyzed in the literature by considering the eigenvalues of small signal linearized models with powers as state variables, see among others [11], [4], [12]. Dynamic phasor models [13] have been used in [14], [15] as the base models for the stability analysis on the corresponding linearized systems. Unfortunately the small signal approximation is often not satisfied in practice. The typically wide operating conditions of distributed generation systems motivate a more detailed stability analysis possibly valid also for large signals. This paper proposes a technique for the estimation of the domain of attraction of the stable equilibrium point for grid-connected droop controlled inverters, by using as methodological ingredients dynamic phasor models [16], singular perturbations [17] and contraction theory [18].

The rest of the paper is organized as follows. In Section II some preliminary definitions and concepts of droop control and dynamic phasors are presented. The dynamic phasor framework allows to write the closed loop dynamic model in a closed form. In Section III the contraction theory applied to that model allows to estimate the domain of attraction of the stable equilibrium point. Section IV presents some insights for the extension of the proposed analysis to the case of multiple inverters in islanded configuration. The numerical results reported in Section V demonstrate the effectiveness of the proposed analysis. Section VI concludes the paper.

II. Dynamic Phasor Model under Droop Control

An equivalent circuit representing H grid-connected inverters is shown in Fig. 1. The voltage generated by the h-th inverter is u_h with $h = 1, \ldots, H$. The grid is modeled as an ideal sinusoidal voltage source v. The h-th inverter is connected to the grid through an equivalent resistive (R_h) and inductive (L_h) impedance, which can also include the virtual impedances generated by the inner loops of the inverter controller. The equivalent scheme can be used for the analysis of both single phase and three phase droop controlled inverters. Since the grid is modeled as an ideal voltage source, the entire model can be separated into H decoupled submodels. Therefore for notational simplicity in the sequel the subscript 'h' will be omitted.

By applying the Kirchhoff Voltage Law to the h-th loop of the circuit in Fig. 1 the corresponding dynamic model can be written as

$$L\frac{d}{dt}i = -Ri + u - v. \tag{1}$$

Department of Engineering, University of Sannio, Piazza Roma 21, 82100 Benevento, Italy, valerio.mariani@unisannio.it, vasca@unisannio.it

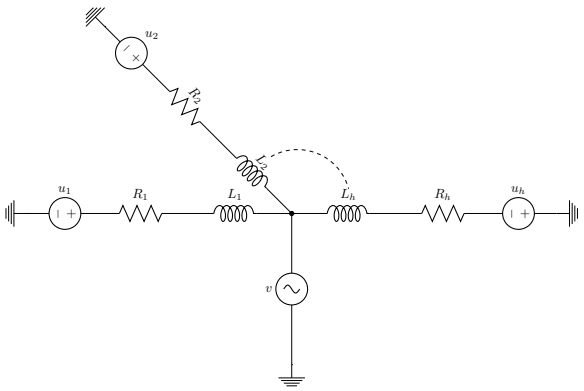

Fig. 1. Equivalent electrical circuit of H grid-connected parallel inverters.

where i is the current and the time dependence of i, u and v have been omitted. The model (1) is linear and time invariant with measurable state variable. Therefore from the system theory perspective the control and the stability analysis of such a system is a trivial problem. On the other hand the model becomes significant for the problem under investigation because, in spite of its simplicity and by means of its correspondent dynamic phasor representation, it allows to develop a stability analysis for the power system with inverter subject to the *nonlinear* droop control. Indeed, equivalent circuits similar to that shown in Fig. 1 have been extensively adopted in the literature for the droop control analysis [5], [6], [7], [10], [19], [15].

The voltage supplied by the inverter can be written as

$$u = \sqrt{2}\, U \cos\theta \tag{2}$$

where $U > 0$ is the amplitude and θ is the instantaneous phase of the inverter voltage. Both U and θ will be determined by the droop controller. The grid voltage can be written as

$$v = \sqrt{2}\, V \cos(\theta - x), \tag{3}$$

where V is the grid voltage amplitude and x is the phase delay between the inverter and the grid voltages. With the definitions above one can write

$$\frac{d}{dt}(\theta - x) = \omega, \tag{4}$$

where ω is the constant and known frequency of the grid.

The definition of a dynamic phasor requires the choice of a reference time-varying angle. In what follows the reference angle is chosen to be θ, i.e., the phase of the inverter voltage. This choice is different from the typical choice adopted for the dynamic phasor models of power systems, where the grid voltage phase ωt is usually considered as the reference angle. Instead, the selection of the "local" inverter angle will allow to write in closed form the dynamic model under droop control and will also ensure the model modularity useful for the case of multiple inverters. From (3), the dynamic phasor $\hat{V}$ associated to the signal v is defined as the complex time–varying signal

$$\hat{V} = V_R + \jmath V_I = V e^{-\jmath x}, \tag{5}$$

where V_R and V_I are the real and imaginary parts of $\hat{V}$ respectively. From (3) the original signal v can be obtained by taking the real part of $\hat{V} e^{\jmath\theta}$:

$$v = \sqrt{2}\, \mathfrak{Re}\{\hat{V} e^{\jmath\theta}\}. \tag{6}$$

According to (2) and the definition (5), since the reference phase is θ, the dynamic phasor $\hat{U}$ will be real, i.e.

$$\hat{U} = U_R = U. \tag{7}$$

Similarly to (6), the original signal u can be recovered from $\hat{U}$ by using

$$u = \sqrt{2}\, \mathfrak{Re}\{\hat{U} e^{\jmath\theta}\}. \tag{8}$$

The dynamic phasor $\hat{I}$ of the current i is defined as

$$\hat{I} = z_R + \jmath z_I = I e^{-\jmath\phi}, \tag{9}$$

where ϕ is the time-varying angle delay of i with respect to θ, z_R and z_I are the real and imaginary parts of $\hat{I}$, respectively, and the signal i can be obtained from $\hat{I}$ by using

$$i = \sqrt{2}\, \mathfrak{Re}\{\hat{I} e^{\jmath\theta}\}. \tag{10}$$

The choice of the notations z_R and z_I to indicate the real and imaginary parts of $\hat{I}$ will be clear in the sequel. By using (6), (8) and (10) in (1), the dynamic model can be equivalently reformulated in terms of the dynamic phasors:

$$\mathfrak{Re}\left\{\left(L\frac{d}{dt}\hat{I} + \jmath L\hat{I}\frac{d}{dt}\theta + R\hat{I} - \hat{U} + \hat{V}\right) e^{\jmath\theta}\right\} = 0. \tag{11}$$

The equation (11) must be satisfied for any $\theta \in [0, 2\pi)$, and therefore is equivalent to

$$L\frac{d}{dt}\hat{I} + \jmath L\hat{I}\frac{d}{dt}\theta + R\hat{I} - \hat{U} + \hat{V} = 0. \tag{12}$$

The amplitude U and the phase θ of the inverter voltage are determined by means of the droop control. In order to present the basic principle of this technique it is useful to recall how the classical concepts of active power and reactive power can be extended to the dynamic phasors domain. Let us define

$$P = \mathfrak{Re}\{\hat{U}\hat{I}^*\}, \tag{13a}$$

$$Q = \mathfrak{Im}\{\hat{U}\hat{I}^*\}, \tag{13b}$$

where the superscript '$*$' is used to indicate the complex conjugate. At steady-state

$$\frac{d}{dt}\hat{I} = 0, \quad \frac{d}{dt}\theta = \omega, \tag{14}$$

and (13) correspond to the classical definitions of active and reactive powers. By considering (7) and (12) at steady-state, (13) become

$$P = \frac{U}{Z^2}[R(U - V\cos x) + \omega L V \sin x], \tag{15a}$$

$$Q = \frac{U}{Z^2}[\omega L(U - V\cos x) - RV\sin x], \tag{15b}$$

where $Z = \sqrt{R^2 + (\omega L)^2}$. The power flow equations for purely inuctive lines can be obtained from (15a) and (15b) with $R = 0$ and $Z = \omega L$:

$$P = \frac{V}{\omega L} U \sin x \approx \frac{V}{\omega L} U x, \tag{16a}$$

$$Q = \frac{1}{\omega L} U (U - V \cos x) \approx \frac{1}{\omega L} U (U - V), \tag{16b}$$

where the approximation is for $|x| \ll 1$. From (16) it is clear that for purely inductive lines the approximated active power P depends on the angle delay between the inverter voltage u and the grid voltage v, while the approximated reactive power Q depends on the difference between U and V without an explicit dependence on x.

The droop control principle is inspired by the decoupling feature of (16): the reactive power can be controlled by acting on U and the active power can be controlled through x. More involved equations can be derived from (15)–(16) in order to apply a similar decoupling principle in the case of non-purely inductive lines. In droop controlled inverters, the angle θ and the amplitude U of the inverter voltage u are then obtained through the following droop equations

$$\frac{d}{dt}\theta = \omega + m(\bar{P} - P), \tag{17a}$$

$$U = \bar{U} + n(\bar{Q} - Q), \tag{17b}$$

where P and Q are given by (13) with (12), $\bar{U}$, $\bar{P}$, $\bar{Q}$ are the inverter's voltage, the active and reactive power references respectively, m and n are the droop control parameters.

It is now possible to determine a closed form for the dynamic phasor model of the droop controlled system. By considering (17a) and (12) with (4), (5) and (7) one obtains

$$\frac{d}{dt}x = m(\bar{P} - P), \tag{18a}$$

$$L\frac{d}{dt}\hat{I} = -(R + \jmath\omega L)\hat{I} - \jmath\frac{d}{dt}x\, L\hat{I} + U - Ve^{-\jmath x}. \tag{18b}$$

By using (9), the current equation (18b) can be split into its real and imaginary parts:

$$L\frac{d}{dt}z_R = -Rz_R + \omega L z_I + m(\bar{P} - P)Lz_I + U - V\cos x, \tag{19a}$$

$$L\frac{d}{dt}z_I = -\omega L z_R - Rz_I - m(\bar{P} - P)Lz_R + V\sin x. \tag{19b}$$

We need now to eliminate the variables P and U from (18a) and (19). By using (7) and (9) in (13), one obtains

$$P = \mathfrak{Re}\{U\hat{I}^*\} = Uz_R, \tag{20a}$$

$$Q = \mathfrak{Im}\{U\hat{I}^*\} = -Uz_I. \tag{20b}$$

Note that the simplicity of the expressions (20) is due to the choice of the inverter phase θ as the reference angle for the dynamic phasor representation. By substituting (20b) in (17b), and by computing U from the resulting equation it follows

$$U = \frac{\bar{U} + n\bar{Q}}{1 - nz_I}. \tag{21}$$

Then (20a) can be rewritten as

$$P = \frac{\bar{U} + n\bar{Q}}{1 - nz_I} z_R. \tag{22}$$

Finally, the closed loop model can be obtained by substituting (21) and (22) in (18a) and (19):

$$\frac{d}{dt}x = m\left(\bar{P} - \frac{\bar{U} + n\bar{Q}}{1 - nz_I} z_R\right), \tag{23a}$$

$$L\frac{d}{dt}z_R = -Rz_R + X_L z_I + m\left(\bar{P} - \frac{\bar{U} + n\bar{Q}}{1 - nz_I} z_R\right) Lz_I + \frac{\bar{U} + n\bar{Q}}{1 - nz_I} - V\cos x, \tag{23b}$$

$$L\frac{d}{dt}z_I = -X_L z_R - Rz_I - m\left(\bar{P} - \frac{\bar{U} + n\bar{Q}}{1 - nz_I} z_R\right) Lz_R + V\sin x, \tag{23c}$$

where $X_L = \omega L$. For sufficiently small values of the inductance L, the model (23) is in the so called singular perturbation form [17] with x being the slow variable, z_R and z_I the fast variables and L the small parameter. Note that the assumption of L being small does not imply that X_L is small too.

III. Stability Analysis

In this section the stability of the model (23) is analyzed by using the contraction theory. In order to recall the contracting region concept let us consider a state space model in the form

$$\frac{d}{dt}\hat{x} = \hat{f}(\hat{x}) \tag{24}$$

with initial condition $\hat{x}_0$ and $\hat{f}(\hat{x}) : \mathbb{R}^n \to \mathbb{R}^n$ being smooth. A subset $\mathcal{C} \subset \mathbb{R}^n$ of the state space is said contracting region if the symmetric part of the Jacobian matrix *function* is negative definite:

$$\mathcal{C} \triangleq \left\{ \hat{x} \in \mathbb{R}^n : \frac{1}{2}\left(\frac{\partial \hat{f}(\hat{x})}{\partial \hat{x}} + \frac{\partial \hat{f}(\hat{x})}{\partial \hat{x}}^T\right) \leq -\beta I \right\}, \tag{25}$$

with $\beta > 0$ and I being the identity matrix [18].

The contracting region has an interesting interpretation. Consider an initial condition $\hat{x}_0^{(1)} \in \mathcal{C}$ and the corresponding trajectory, say $\hat{x}^{(1)}(t)$, generated by (24). If one can find a ball $\mathcal{B}(t)$ centered in $\hat{x}^{(1)}(t)$ and such that $\mathcal{B}(t) \subset \mathcal{C}$ for all $t \geq 0$, then any other trajectory $\hat{x}^{(2)}(t)$ given by the initial condition $\hat{x}_0^{(2)} \in \mathcal{B}(0)$ remains in $\mathcal{B}(t)$ for all $t > 0$ and, further, the difference $\hat{x}^{(2)}(t) - \hat{x}^{(1)}(t)$ exponentially converges to zero as the time t tends to infinity. A similar converse result holds, see [18]. If $\hat{x}_0^{(1)} \in \mathcal{C}$ is an equilibrium point, then the contracting region, if exists, it represents an estimate of the domain of attraction, which is defined as the set of initial conditions around $\hat{x}_0^{(1)}$ such that the corresponding trajectories converge to that equilibrium, but not necessarily exponentially, e.g., with polynomial rate.

We are now ready to prove that the slow subsystem obtained from the droop controlled system is contracting. The following theorem provides also an expression for the estimate of the contracting region.

Theorem 1: Consider the system (23). The slow subsystem obtained from (23) by considering L as a small parameter can be written in the following differential algebraic equation form

$$\frac{d}{dt}x_s = f(x_s, U_s), \tag{26a}$$

$$0 = g(x_s, U_s), \tag{26b}$$

where $g(x_s, U_s)$ defines a unique mapping $U_s(x_s) : [-\pi, \pi) \subset \mathbb{R} \to \mathcal{D}_{U_s} \subseteq \mathbb{R}^+$. Moreover, the region defined by

$$\mathcal{C} = \left\{ x_s \in [-\pi, \pi) : \left(2U_s(x_s) + \frac{X_L}{n}\right)\cos x_s + \frac{R}{n}\sin x_s - V > 0 \right\}, \tag{27}$$

where

$$U_s(x_s) = -\frac{\xi(x_s)}{2} + \sqrt{\frac{\xi^2(x_s)}{4} + \frac{Z^2}{nX_L}(\bar{U} + n\bar{Q})}, \tag{28}$$

and

$$\xi(x_s) = \frac{Z^2}{nX_L} - \frac{RV}{X_L}\sin x_s - V\cos x_s, \tag{29}$$

is a contracting region for (26).

Proof: By assuming $L = 0$ in (23) it follows

$$\frac{d}{dt}x_s = m\left(\bar{P} - \frac{\bar{U} + n\bar{Q}}{1 - n\bar{z}_I}\bar{z}_R\right), \tag{30a}$$

$$0 = -R\bar{z}_R + X_L\bar{z}_I + \frac{\bar{U} + n\bar{Q}}{1 - n\bar{z}_I} - V\cos x_s, \tag{30b}$$

$$0 = -X_L\bar{z}_R - R\bar{z}_I + V\sin x_s, \tag{30c}$$

where x_s represents the "slow" varying angle and $(\bar{z}_R, \bar{z}_I)$ the steady-state real and imaginary parts of the current's dynamic phasor. Denoting by U_s the slow droop controlled voltage, from (21) it follows

$$U_s = \frac{\bar{U} + n\bar{Q}}{1 - n\bar{z}_I}, \tag{31}$$

and (30) can be rewritten in the form (26):

$$\frac{d}{dt}x_s = m\left(\bar{P} + \frac{R}{nX_L}\left(U_s - (\bar{U} + n\bar{Q})\right) - \frac{V}{X_L}U_s\sin x_s\right), \tag{32a}$$

$$0 = U_s^2 + \left(\frac{Z^2}{nX_L} - \frac{RV}{X_L}\sin x_s - V\cos x_s\right)U_s - \frac{Z^2}{nX_L}(\bar{U} + n\bar{Q}). \tag{32b}$$

For any positive n, (32b) will always have a single real positive root. Then (32b) defines a unique map between the positive U_s and $x_s \in [-\pi, \pi)$. Therefore, by using the implicit function's theorem, the Jacobian function of (26) can be written as

$$J_f = \frac{\partial}{\partial x_s}f(x_s, U_s) + \frac{\partial}{\partial U_s}f(x_s, U_s)\frac{d}{dx_s}U_s \tag{33}$$

where

$$\frac{d}{dx_s}U_s = -\left(\frac{\partial}{\partial U_s}g(x_s, U_s)\right)^{-1}\frac{\partial}{\partial x_s}g(x_s, U_s), \tag{34}$$

and, more specifically

$$\frac{\partial}{\partial x_s}f(x_s, U_s) = -\frac{mV}{X_L}U_s\cos x_s, \tag{35a}$$

$$\frac{\partial}{\partial U_s}f(x_s, U_s) = \frac{m}{X_L}\left(\frac{R}{n} - V\sin x_s\right), \tag{35b}$$

$$\frac{\partial}{\partial x_s}g(x_s, U_s) = \left(-\frac{RV}{X_L}\cos x_s + V\sin x_s\right)U_s, \tag{35c}$$

$$\frac{\partial}{\partial U_s}g(x_s, U_s) = 2U_s + \left(\frac{Z^2}{nX_L} - \frac{RV}{X_L}\sin x_s - V\cos x_s\right). \tag{35d}$$

From (32b) and (35d) one obtains

$$\frac{\partial}{\partial U_s}g(x_s, U_s) = U_s + \frac{1}{U_s}\frac{Z^2}{nX_L}(\bar{U} + n\bar{Q}) > 0, \tag{36}$$

then by using (34) and (35) in (33) and by exploiting (36), it follows that (33) being negative is equivalent to

$$\left[2U_s + \left(\frac{Z^2}{nX_L} - \frac{RV}{X_L}\sin x_s - V\cos x_s\right)\right]\cos x_s + \left(-\frac{R}{X_L}\cos x_s + \sin x_s\right)\left(\frac{R}{n} - V\sin x_s\right) > 0. \tag{37}$$

Then, the region $\mathcal{C}$ defined by (27)–(29) is a contracting region for (32). ∎

The numerical results in Section V will show that Theorem 1 provides a good estimate for the region of attraction of the desired equilibrium point under droop control.

Notice that, though the model (23) has been obtained by considering a single phase equivalent circuit, it is simple to show that the same model represents also an analogous balanced three phase circuit where the real and imaginary components of the dynamic phasor are replaced by the direct and quadrature currents represented in a reference frame synchronous with the inverter voltage [20]. In particular for the three phase case the direct and quadrature components can be obtained by applying a Park transformation and a rotation on the measured instantaneous signals.

IV. Multiple Islanded Inverters

The procedure for the construction of the dynamic phasor model for grid-connected inverters can be also applied to the case of multiple islanded inverters, whose scenario corresponds to the equivalent circuit depicted in Fig. 1 where the voltage source representing the grid is replaced by a generic resistive (R) and inductive (L) load. In this case the voltage v represents the voltage on the common load which is not constrained by the grid. By using the same approach presented in Section II the dynamic phasor of the voltage of each inverter is represented with respect to its local phase reference, say θ_h for the inverter voltage u_h and θ_v for the load voltage:

$$u_h = \sqrt{2}U_h\cos\theta_h, \tag{38a}$$

$$v = \sqrt{2}V\cos\theta_v = \sqrt{2}V\cos(\theta_h - x_h), \tag{38b}$$

with the following equation defining x_h

$$\frac{d}{dt}(\theta_h - x_h) = \frac{d}{dt}\theta_v = \omega_v, \tag{39}$$

and ω_v is unknown. By applying the Kirchhoff Voltage and Current Laws one obtains

$$L_h \frac{d}{dt} i_h = -R_h i_h + u_h - v, \tag{40a}$$

$$L \frac{d}{dt} i = -Ri + v, \tag{40b}$$

$$i = \sum_{h=1}^{H} i_h, \tag{40c}$$

where $h = 1, \ldots, H$, and the voltage u_h of the h-th inverter is subject to the droop equations

$$\frac{d}{dt}\theta_h = \omega + m_h(\bar{P} - P_h), \tag{41a}$$

$$U_h = \bar{U} + n_h(\bar{Q} - Q_h). \tag{41b}$$

By using arguments similar to those presented in Section II it simple to determine the following model

$$\frac{d}{dt} x_h = \omega - \omega_v + m_h(\bar{P} - P_h), \tag{42a}$$

$$L_h \frac{d}{dt}\hat{I}_h = -(R_h + \jmath\omega L_h)\hat{I}_h - \jmath m_h(\bar{P} - P_h) L_h \hat{I}_h + U_h - V e^{-\jmath x_h}, \tag{42b}$$

$$L \frac{d}{dt}\hat{I} = -(R + \jmath\omega_v L)\hat{I} + V, \tag{42c}$$

$$\hat{I} = \sum_{h=1}^{H} \hat{I}_h e^{\jmath x_h}, \tag{42d}$$

with

$$U_h = \frac{\bar{U} + n_h \bar{Q}}{1 - n_h z_{I,h}}, \tag{43a}$$

$$P_h = \frac{\bar{U} + n_h \bar{Q}}{1 - n_h z_{I,h}} z_{R,h}. \tag{43b}$$

The dynamic model (42) represents $3H + 4$ real equations in terms of the following $3H + 4$ real unknowns: x_h (H variables), $\hat{I}_h$ ($2H$ variables), $\hat{I}$ (2 variables), V (1 scalar variable) and ω_v (1 scalar variable). Note that ω is a known parameter, θ_v does not appear in the equations, and the synchronization frequency ω_v is not fixed a priori. The differential algebraic structure of the model for islanded inverters suggests the possibility of a stability analysis through arguments similar to those presented in Section III. This is a direction for future research.

V. Simulation Results

The simulations have been carried out by considering the following nominal values of the control and line parameters: $n = 10^{-4}$ V/VAr, $m = 10^{-4}$ rad/sW, $\bar{P} = 1005$ W, $\bar{Q} = 525$ VAr, $\bar{U} = 223$ V, $V = 220$ V, $R = 0.2\ \Omega$, $X_L = 1\ \Omega$, $\omega = 2\pi\, 60$ rad/s. The equilibrium points of (32) are $(x_{s,1}^{\mathrm{eq}}, U_{s,1}^{\mathrm{eq}}) = (0.018, 223)$ and $(x_{s,2}^{\mathrm{eq}}, U_{s,2}^{\mathrm{eq}}) = (-2.77, 214)$. It is simple to demonstrate that $(x_{s,2}^{\mathrm{eq}}, U_{s,2}^{\mathrm{eq}})$ is an unstable equilibrium point. The contracting region, corresponding to $(x_{s,1}^{\mathrm{eq}}, U_{s,1}^{\mathrm{eq}})$, estimated by using Theorem 1, is $\mathcal{C} = (-1.36, 1.74)$. The open set $\mathcal{B} = (-1.36, 1.396)$ centered in $x_{s,1}^{\mathrm{eq}}$ is contained (at any time) in $\mathcal{C}$. By using the contraction theory, any trajectory $x_s^{(i)}(t)$ such that the initial condition $x_{s,0}^{(i)} \in \mathcal{B}$ will exponentially converge to $x_{s,1}^{\mathrm{eq}}$, and $\mathcal{B}$ represents an estimate of the domain of attraction of $x_{s,1}^{\mathrm{eq}}$. Fig. 2 shows the exponential convergence to the equilibrium point $x_{s,1}^{\mathrm{eq}} = 0.018$ of the angle x_s for different initial conditions inside and outside $\mathcal{B}$. This result is confirmed by the simulations carried out by using the full order model (23), see Fig. 3.

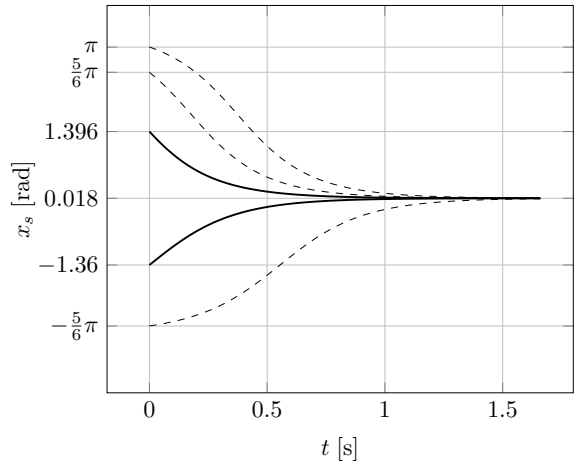

Fig. 2. Evolution of x_s for different initial conditions. The thick line represents the trajectories starting at the boundaries of $\mathcal{B}$ while the dashed line represents the trajectories starting outside $\mathcal{B}$.

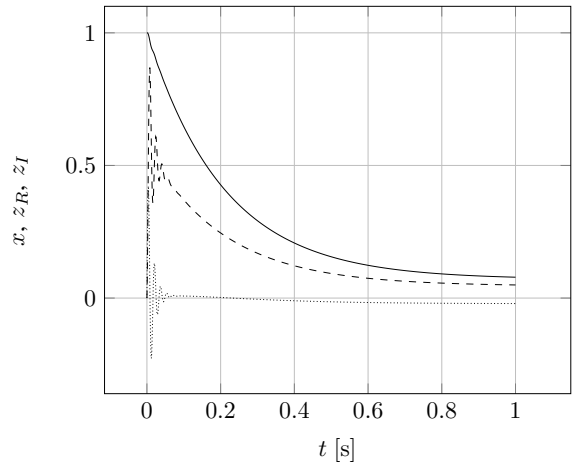

Fig. 3. Angle x (solid line), direct z_R (dashed line) and quadrature z_I (dotted line) currents of (23) in p.u. with respect to $\pi/12$ rad for x and 100 A for z_R and z_I.

The presence of slow and fast modes in (23) depends on the control parameter m, so as it might be conjectured from (23a). Fig. 4 shows that a sufficiently small m will ensure a dynamic separation of one order of magnitude between the modes of the linearized system. Fig. 5 shows the sensitivity of the contracting region $\mathcal{C}$ estimated through Theorem 1 with respect to L and n.

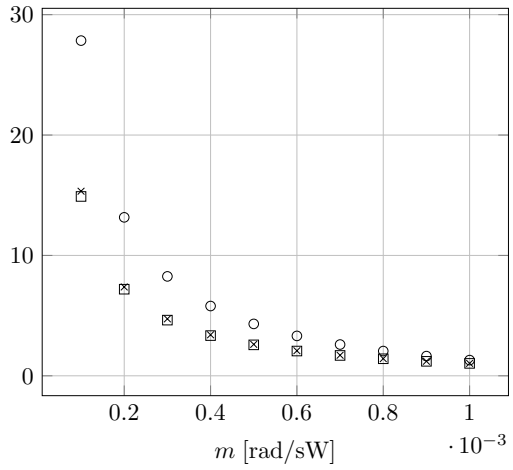

Fig. 4. Ratio between the real part of the complex eigenvalue and the real eigenvalue of the linearized system from (23) around the equilibrium points corresponding to $m \in [10^{-4}, 10^{-3}]$ and $L = 5L^{\rm nom}$ (circle), $L = L^{\rm nom}$ (cross) and $L = L^{\rm nom}/5$ (square).

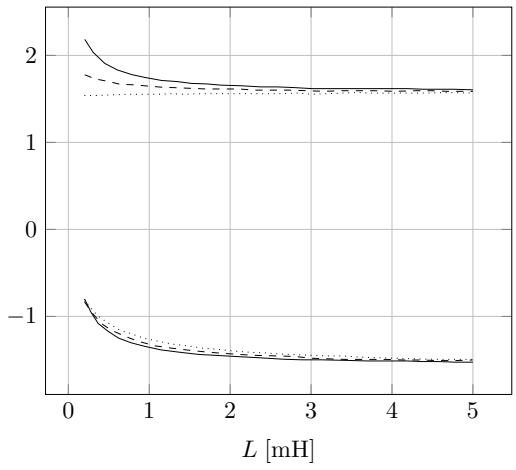

Fig. 5. Boundaries of the contracting region $\mathcal{C}$ with respect to the line inductance $L \in [L^{\rm nom}/5, 5L^{\rm nom}]$ for $n = 10^{-4}$ (solid line), $n = 5 \times 10^{-4}$ (dashed line) and $n = 10^{-3}$ (dotted line).

VI. Conclusions

The dynamic phasor model of an inverter subject to droop control and connected to the grid, for a realistic set of parameters, highlights a clear dynamic separation between the fast currents and the slow angle time evolutions. The use of the singular perturbation technique allows to discuss the stability of the system by considering the simpler reduced order dynamic model. The application of the contraction theory provides an estimate of the domain of attraction of the exponentially stable equilibrium point. The simulation results have confirmed the theoretical analysis.

Directions of future research are the application of the proposed stability analysis to the dynamic phasor model for parallel inverters in islanded modes and the stability analysis for the fast subsystem.

References

[1] T. Kawabata and S. Higashino, "Parallel operation of voltage source inverters," *IEEE Transactions on Industry Applications*, vol. 24, no. 2, pp. 281–297, 1988.

[2] J. M. Guerrero, J. C. Vasquez, J. Matas, L. G. de Vicuña, and M. Castilla, "Hierarchical control of droop-controlled AC and DC microgirds — a general approach toward standardization," *IEEE Transactions on Industrial Electronics*, vol. 58, no. 1, pp. 156–172, 2011.

[3] Y. Zhang and H. Ma, "Theoretical and experimental investigation of networked control for parallel operation of inverters," *IEEE Transactions on Industrial Electronics*, vol. 59, no. 4, pp. 1961–1970, 2012.

[4] M. B. Delghavi and A. Yazdani, "An adaptive feedforward compensation for stability enhancement in droop-controlled inverter-based microgrids," *IEEE Transactions on Power Delivery*, vol. 26, no. 3, pp. 1764–1773, 2011.

[5] K. D. Brabandere, B. Bolsens, J. van den Keybus, A. Woyte, J. Driesen, and R. Belmans, "A voltage and frequency droop control method for parallel inverters," *IEEE Transactions on Power Electronics*, vol. 22, no. 4, pp. 1107–1115, 2007.

[6] S. V. Iyer, M. N. Belur, and M. C. Chandorkar, "Decentralized control of a line interactive uninterruptible power supply (UPS)," in *Proc. of American Control Conference*, Baltimore, MD, USA, July 2010, pp. 3293–3298.

[7] J. M. Guerrero, L. G. de Vicuña, J. Matas, M. Castilla, and J. Miret, "A wireless controller to enhance dynamic performance of parallel inverters in distibuted generation systems," *IEEE Transactions on Power Electronics*, vol. 19, no. 5, pp. 1205–1213, 2004.

[8] J. M. Guerrero, J. Matas, L. G. de Vacuña, M. Castilla, and J. Miret, "Wireless-control strategy for parallel operation of distributed-generation inverters," *IEEE Transactions on Industrial Electronics*, vol. 53, no. 5, pp. 1461–1470, 2006.

[9] J. C. Vasquez, J. M. Guerrero, A. Luna, P. Rodriguez, and R. Teodorescu, "Adaptive droop control applied to voltage-source inverters operating in grid-connected and islanded modes," *IEEE Transactions on Industrial Electronics*, vol. 56, no. 10, pp. 4088–4096, 2009.

[10] W. Yao, M. Chen, J. Matas, J. M. Guerrero, and Z. M. Qian, "Design and analysis of the droop control method for parallel inverters considering the impact of the complex impedance on the power sharing," *IEEE Transactions on Industrial Electronics*, vol. 58, no. 2, pp. 576–588, 2011.

[11] J. M. Guerrero, J. C. Vásquez, J. Matas, M. Castilla, and L. G. de Vacuña, "Control strategy for flexible microgrid based on parallel line-inductive UPS systems," *IEEE Transactions on Industrial Electronics*, vol. 56, no. 3, pp. 726–736, 2009.

[12] Y. Mohamed and E. El-Saadany, "Adaptive decentralized droop cotroller to preserv power sharing stability of paralleled inverters in distributed generation microgrids," *IEEE Transactions on Power Electronics*, vol. 23, no. 6, pp. 2806–2816, 2008.

[13] S. R. Sanders, J. M. Noworolski, X. Z. Liu, and G. C. Verghese, "Generalized averaging method for power conversion circuits," *IEEE Transactions on Power Electronics*, vol. 6, no. 2, pp. 251–259, 1991.

[14] S. Bala and G. Venkataramanan, "On the choice of voltage regulators for droop-controlled voltage source converters in microgrids to ensure stability," in *Proc. of IEEE Energy Conversion Congress and Exposition*, Atlanta, GA, USA, September 2010, pp. 3448–3455.

[15] X. Wang, F. Zhuo, H. Guo, L. Meng, M. Yang, and J. Liu, "Stability analysis of droop control for inverter using dynamic phasors method," in *Proc. of IEEE Energy Conversion Congress and Exposition*, Phoenix, AZ, USA, September 2011, pp. 739–742.

[16] S. Almér and U. Jönsson, "Harmonic analysis of pulse-width modulated systems," *Automatica*, vol. 45, no. 4, pp. 851–862, 2009.

[17] H. K. Khalil, *Nonlinear Systems*, 3rd ed. New Jersey: Prentice Hall, 2002.

[18] W. Lohmiller and J.-J. E. Sotine, "On contraction analysis for nonlinear systems," *Automatica*, vol. 34, no. 6, pp. 683–696, 1998.

[19] S. Dasgupta, S. K. Sahoo, and S. K. Panda, "Single-phase inverter control techniques for interfacing renewable energy sources with micrgrid — part I: Parallel-connected inverter topology with active and reactive power flow control along with grid current shaping," *IEEE Transactions on Power Electronics*, vol. 26, no. 3, pp. 717–731, 2011.

[20] C. Di Pietro, F. Vasca, L. Iannelli, and F. Oliviero, "Decentralized synchronization of parallel inverters for train auxiliaries," in *Proc. of Electrical Systems for Aircraft, Railway and Ship Propulsion*, Bologna, Italy, October 2010, pp. 1–6.